Hydrogels Based on Dual Curable Chitosan-*graft*-Polyethylene Glycol-*graft*-Methacrylate: Application to Layer-by-Layer Cell Encapsulation

Yin Fun Poon, Ye Cao, Yunxiao Liu, Vincent Chan, and Mary B. Chan-Park*

School of Chemical and Biomedical Engineering, Nanyang Technological University, 62 Nanyang Drive, Singapore 637459, Singapore

ABSTRACT Ultraviolet (UV) photo-cross-linkable hydrogels have been commonly used for three-dimensional (3D) encapsulation of cells. Previous UV cross-linkable hydrogels have employed one-shot hardening of mixtures of hydrogels and cells. Here we propose an alternative method of making hydrogel-encapsulated cell constructs through layer by layer (LBL) buildup of alternating layers of cells and hydrogel. The LBL method potentially permits better spatial control of different cell types and control of cell orientation. Each hydrogel layer must be hardened before deposition of the next layer of cells. A UV-curable gel precursor that can also be gelled at physiological temperature is desirable to avoid repeated UV exposure of cells after deposition of each successive hydrogel layer. We designed, synthesized, and applied such a precursor, dual-curable—both thermoresponsive and UV-curable—chitosan-*graft*-polyethylene glycol-*graft*-methacrylate (CEGx-MA) copolymer (x is the PEG molecular weight in Daltons). We found that CEG350-MA copolymer solutions (5 wt % polymer) formed physical gels at ~37 °C and could be further photopolymerized to form thermally stable dual-cured hydrogels. This material was applied to the creation of a two-layer LBL smooth muscle cell (SMC)/hydrogel construct using temperature elevation to ~37 °C to gel each hydrogel layer. The physically gelled two-layered hydrogel/cell construct was finally exposed to a single UV shot to improve its mechanical properties and render it thermally stable. CEG350-MA solution and gel are nontoxic to SMCs. Cells remained mostly viable when they were encapsulated inside both physically gelled and dual-cured CEG350-MA and suffered little damage from the single brief UV exposure. The combination of LBL tissue engineering with a dual curable hydrogel precursor such as CEG350-MA permits the buildup of viable thick and complex tissues in a stable, biocompatible, and biodegradable matrix.

KEYWORDS: chitosan • polyethylene glycol • hydrogels • photopolymerization • smooth muscle cells

1. INTRODUCTION

Hydrogels are three-dimensional (3D) networks of hydrophilic polymers which can preserve large amount of water in their structures. Their compositions can be tuned to achieve physical characteristics resembling those of biological tissues for applications in cell delivery and encapsulation (1–4). Hydrogels have been used as synthetic extracellular matrices (ECMs) for encapsulating cells in tissue engineering (1, 5, 6). We (7, 8) and others (9, 10) have shown that cells can be encapsulated inside ultraviolet (UV) photo-cross-linked hydrogels with high viability and proliferation rate. Previous reports (1, 5–10) involving UV cross-linked hydrogels for 3D cell encapsulation have applied one-shot UV hardening of mixtures of hydrogels and cells. Limitations of one-shot UV photo-cross-linking include low cell density, poor control of cell alignment and phenotype, etc. (11).

Here, we propose an alternative approach to the construction of thick multilayered tissue through a LBL hydrogel encapsulation of cells. The LBL technique has been used to construct biomimetic native-like three-dimensional tissue. Mjahed et al. and Grossin et al. prepared LBL scaffold consisting of alternating layers of cell-containing alginate and multilayered film which comprises polyanion and poly(L-lysine) (12, 13). The cells embedded within the alginate gels were viable and the polyelectrolyte multilayer can encapsulate bioactive molecules like growth factors within them (13).

In our approach, a first layer of cells is grown on a surface to confluence and then a hydrogel precursor solution is deposited over the confluent cells and then hardened (Scheme 1). A second layer of cells is grown on top of the first layer of hardened hydrogel followed by hardening of a second hydrogel layer on the second layer of cells; the alternate deposition of cells and hydrogel is repeated several times to build a thick tissue. The LBL cell/hydrogel buildup can potentially allow higher density, better alignment of cells or construction of multicell type tissues. However, repeated exposure of cells to UV light is known to be harmful so that application of multiple UV exposures to harden each successive layer in turn for buildup of thick tissues with LBL is infeasible. Other methods of gel hardening are needed for the LBL encapsulation of cells (14, 15). One such alternative hardening method involves thermally responsive gels. Com-
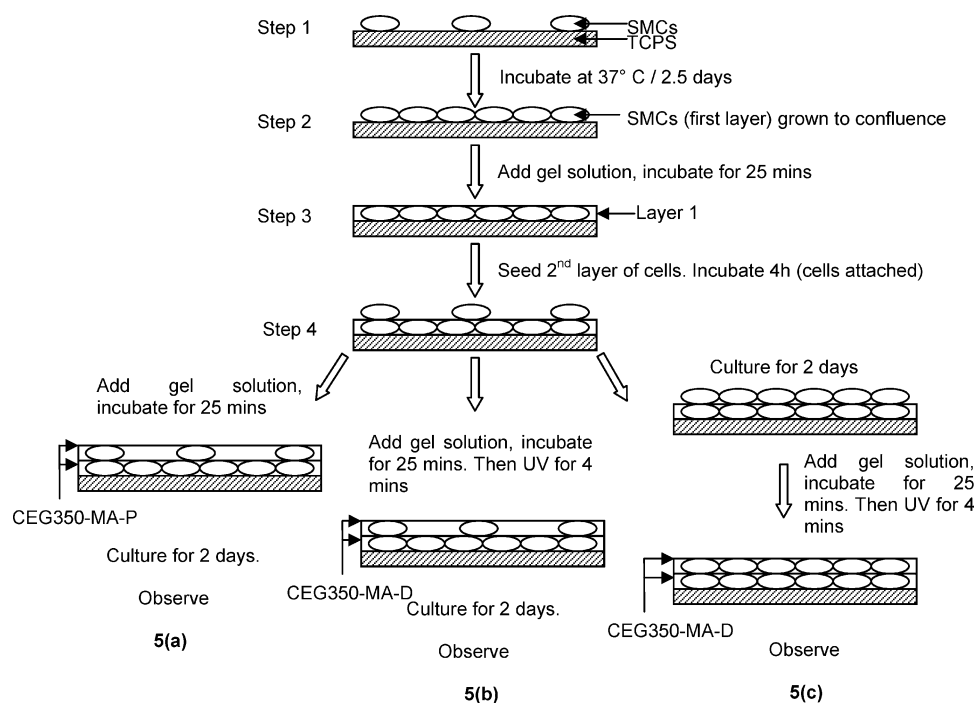
Scheme 1. Schematic for LBL Cell Culture

mon thermoresponsive gels include those based on *N*-isopropylacrylamide (16, 17) and Pluronic (18, 19). However, thermoresponsive hydrogels are typically thermoreversible so that they revert to sol when the temperature is lowered. Hydrogels suitable for tissue engineering applications should also be stable against temperature variations for ease of handling. We propose a dual-curable hydrogel that is thermoresponsive as well as UV photo-cross-linkable. Each hydrogel layer can be separately hardened after application by raising the temperature so as to build up multiple alternating layers of hydrogel and cells. The entire hydrogel/cell construct can then be UV photopolymerized to make it more thermally stable. In this way, the cell layers are built up by LBL but are subjected to UV only once.

Chitosan, a cationic polysaccharide of *D*-glucosamine and *N*-acetyl-*D*-glucosamine, is known to be biocompatible, nontoxic, antibacterial, and biodegradable (20−22). Thermoresponsive copolymers of chitosan and *N*-isopropylacrylamide, poly(vinyl alcohol), poly(ethylene glycol) (PEG), etc., have been reported (23−30). Most of these systems can undergo a sol−gel transition at temperatures close to the physiological temperature of 37 °C. Bhattarai et al. (31, 32) have reported that solutions of PEG-grafted chitosan were able to gel at 37 °C and the gel has been used for in vitro drug release (31). However, there are few reports on thermoresponsive copolymers of chitosan and PEG, which is also biocompatible (31, 32). A nonthermoresponsive chitosan-PEG hydrogel network based on blending chitosan acrylate and thiol-terminated PEG star polymer has been prepared and applied in cell encapsulation (33). As far as we know, there is no reported work on application of thermoresponsive chitosan-*graft*-PEG as cell carrier or encapsulant. There is also no reported work on dual-cure hydrogel systems based on chitosan-*graft*-PEG-*graft*-methacrylate, which is both thermoresponsive and photopolymerizable.

In this study, we prepared two chitosan-*graft*-PEG-*graft*-methacrylate copolymers with different PEG molecular weights (M_n) of 350 and 2000 Da; hereafter, we shall refer to these graft copolymers as CEGx, where x denotes the M_n of the PEG. Scheme 2 shows the synthetic strategy. Methacrylate groups were introduced (Scheme 2b) to produce a novel photo-cross-linkable copolymer, chitosan-*graft*-PEG-*graft*-methacrylate (CEGx-MA). These chitosan derivatives were characterized using Fourier transform infrared (FTIR) spectroscopy, ^{1}H nuclear magnetic resonance (NMR) spectroscopy, and elemental analysis to confirm successful substitution. Ninhydrin assay was used to analyze the grafting position. CEGx-MA solutions formed physical gels (hereafter denoted CEGx-MA-P) upon increasing the incubation temperature from 10 to 60 °C. The physical gels were further cross-linked by UV irradiation to produce dual-cured hydrogels (CEGx-MA-D). The rheological and mechanical properties of both the physical and dual-cured gels were investigated. Smooth muscle cells (SMCs) were cultured on both the physical and dual-cured hydrogels (CEGx-MA-P and CEGx-MA-D) for 7 days and the MTT assay was performed. Layer-by-layer cell encapsulation was also performed with CEG350-MA(-P and -D) (Scheme 1).

2. EXPERIMENTAL METHODS

2.1. Materials. Chitosan with number-average molecular weight (M_n) of 1.05×10^5 Dalton was purchased from Dalian Xindie (Chitin) Pte Ltd. Tetrabutyl ammonium bromide, α-methoxy-terminated polyethylene glycol (PEG) of number-averaged molecular weight (M_n) 350 and 2000 Da, *D*-glucosamine, ninhydrin, hydrindanthin, dimethylsulfoxide (DMSO), glycidyl methacrylate, and thiazolyl blue tetrazolium bromide were purchased

Scheme 2. (a) Synthesis of Chlorofunctionalised PEG, Reflux/24 h; (b) Reaction Scheme for Synthesis of CEGx: (i) Grafting of PEG onto Chitosan to form CEGx, NaOH/ClCH$_2$CO(OCH$_2$CH$_2$)$_n$-OCH$_3$/r.t./24−48 h; and (ii) Formation of CEGx-MA, Glycidyl Methacrylate/Et$_3$N/Bu$_4$NH$_4^+$Br$^-$/r.t./2 Days

Chitosan-*graft*-PEG-*graft*-methacrylate (CEGx-MA)
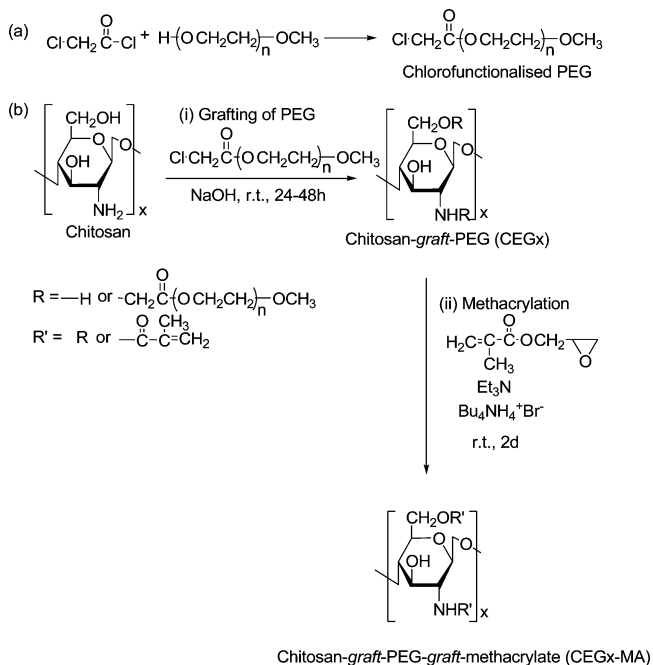
from Aldrich and used as received. Potassium carbonate (anhydrous) and triethylamine were purchased from Fluka and used as received. Sodium hydroxide (NaOH) solution in deionized (DI) water was prepared using sodium hydroxide pellets purchased from Merck. Chloroacetyl chloride was obtained from Merck and reagent grade toluene and analytical grade isopropanol and hydrochloric acid were purchased from Fisher Scientific. Technical grade acetone and ethanol were purchased from VWR (Singapore) and used directly. The photoinitiator, 4-(2-hydroxyethoxy)phenyl-(2-hydroxy-2-propyl) ketone (Irgacure 2959), was purchased from Ciba (Singapore).

2.2. Synthesis. Scheme 2 shows our strategy to synthesize (a) chlorofunctionalized PEG (Cl-PEG) intermediate and (b) CEGx-MA using low and high molecular weight PEG (M_n: 350 or 2000 Da).

2.2.1. *Synthesis of Chlorofunctionalized PEG.* Chlorofunctionalized PEG was synthesized using a method similar to that reported by Reining et al. (34). 7.06 mmol of α-methoxy-terminated PEG dissolved in 100 mL of toluene was added with 28.24 mmol of chloroacetyl chloride. The solution was then heated under reflux for 24 h. After the reaction, the solvents were evaporated under high vacuum and the residue dissolved in 150 mL of dry dichloromethane. Potassium carbonate was added and the mixture was stirred and filtered. Chlorofunctionalised PEG (M_n 2000) is a solid and was purified via precipitation. The solvent in the filtrate was first evaporated and the residue was dissolved in 100 mL of toluene. The solid was then reprecipitated in 750 mL of hexane. The product was obtained after filtration and dried under a vacuum at room temperature. The lower molecular weight chlorofunctionalised PEG (M_n 350) is a liquid and was purified by evaporating the solvent under high vacuum until a thick viscous fluid was obtained.

2.2.2. *Synthesis of Chitosan-graft-PEG (CEG).* 2.0 g of chitosan was added to 25.0 mL NaOH (50 wt %) solution and stirred for 24 h. The resulting slurry was filtered to obtain

alkalized chitosan. Chlorofunctionalized PEG (molar ratio of chitosan monomer unit to PEG added was 1.8:1.0) was dissolved in 25.0 mL of isopropanol and the solution was added dropwise to the alkalized chitosan. The mixture was reacted at room temperature overnight to synthesize CEG350 but for 2 days to synthesize CEG2000. After the reaction, the mixture was filtered and the residue dissolved in 100 mL of water. 2.5 M hydrochloric acid was then added to neutralize the pH of the solution. After centrifugation, the product was precipitated from the supernatant liquid by adding 150 mL of acetone, followed by 150 mL of a 2:1 (v/v) mixture of acetone and ethanol. The product was filtered and left to air-dry at room temperature until constant weight. The chitosan-*g*-PEGs with molecular weight x (CEGx, x = 350 and 2000) obtained were white solids. A molar ratio of chitosan monomer:PEG of 1.8:1.0 was necessary to achieve good water solubility for both, whereas a molar ratio of chitosan monomer to PEG of 2.3:1.0 (lower limit) gave products that were only sparingly soluble in water.

2.2.3. *Methacrylation of CEGx.* One gram of CEGx was first dissolved in 100 mL of distilled water before addition of 230 μL of triethylamine, 150 μL of glycidyl methacrylate, and 0.27 g of tetrabutyl ammonium bromide. The mixture was stirred for 2 days at room temperature. To purify the product, the reacted mixture was dialyzed for at least 3 days to remove toxic unreacted triethylamine and glycidyl methacrylate. Dialysis also removes impurities or unreacted reactants from the previous synthesis steps. The membrane tubing (Spectrum Laboratories) used in the dialysis has a molecular weight cutoff of 3500 Da. The methacrylated CEGx (CEGx-MA) solution was then lyophilized.

2.3. Physical Hydrogel Preparation and Gelation Study. Five weight percent CEGx-MA solutions in phosphate buffered saline (PBS) were prepared in 10-mL glass bottles. The mixtures were stirred and vortexed several times for complete dissolution. The resulting solutions were left overnight at 4 °C before increasing the temperature to physically gel the polymer solution. The glass bottles were placed in a water bath at 37 °C for various time durations (15 min, 25 min, 60 min, and 24 h). The tube-inversion method was used to determine the sol−gel transition (31, 32). Briefly, the tube was first placed in the water bath at 37 °C for 25 min and then removed from the bath and immediately inverted to determine if the solution could flow; if the solution did not flow, a gel had formed.

2.4. Photopolymerization of Physical Gels (Dual-Cured Hydrogels). 0.05 wt % Irgacure 2959 photoinitiator was added to the CEGx-MA (5 wt %) solution. Unless otherwise stated, the solution (150 μL) was then placed into a well of a 24-well cell culture dish, which served as the mold, at 37 °C for 25 min in an incubator; in some cases, the physical gelation was conducted at 37 °C for 24 h. After the physical gel was formed, the gel was exposed to UV light (4 min exposure) using a Honle UV Technology machine equipped with an in-built UV mercury lamp with wavelength of 365 nm and intensity of 10 mW/cm^2.

2.5. RGD Grafting onto CEGx-MA Hydrogels. RGD was immobilized on hydrogels according to a method reported by Zhu et al. (35). Briefly, hydrogels were formed in 96-well cell culture dishes by physical gelation (37 °C for 25 min); some were further immediately photopolymerized (for 4 min). Immediately after preparation, the hydrogels were soaked in 1 wt % of glutaraldehyde solution for 10 h at 4 °C and then rinsed with distilled water to removed unbound glutaraldehyde. The hydrogels were then soaked in 1.0 mg/mL of RGD/PBS solution for 24 h at 4 °C. The RGD-grafted hydrogels were then rinsed twice with PBS to remove ungrafted RGD.

2.6. Characterization. The water solubility test was conducted by mixing 0.010 g of CEGx and CEGx-MA in 1.0 mL PBS. The ninhydrin assay was carried out to determine the -NH$_2$ content (36, 37). Ninhydrin reagent was first prepared by adding 4 M lithium acetate buffer (10 mL) to ninhydrin (0.8 g) and

hydrindanthin (0.12 g) in DMSO (30 mL). The ninhydrin reagent (0.5 mL) and the sample (0.5 mL) were added together in a test tube. The mixture was then heated in boiling water for 30 min and cooled to room temperature. Ethanol and water (5 mL, 50:50 (v/v)) were added to the cooled tubes and then vortexed. The absorbance of the solution was measured with a UV spectrophotometer (Nicolet Evolution 500) at a wavelength of 570 nm. The calibration curve was obtained using different concentrations of D-glucosamine standards.

The degrees of PEG substitution and methacrylation of chitosan and its derivatives were calculated from the mole percentages of carbon and nitrogen in the sample that were determined through elemental analysis (38)

$$\text{DS of PEG group} =$$
$$\frac{\frac{C}{N}\text{mol \% (CEG)} - \frac{C}{N}\text{mol \% (chitosan)}}{\frac{C}{N}\text{mol \% (chitosan)}} \times 100\%$$

$$\text{DS of methacrylate group} =$$
$$\frac{\frac{C}{N}\text{mol \% (CEG-MA)} - \frac{C}{N}\text{mol \% (CEG)}}{\frac{C}{N}\text{mol \% (CEG)}} \times 100\%$$

^{1}H NMR studies were carried out using a Bruker Avance 300 MHz instrument. ^{1}H NMR samples were prepared by dissolving the product in deuterium oxide (D_2O) and were recorded at 40 °C. FTIR spectra of vacuum-dried samples were performed at room temperature using a Digilab FTS 3100 instrument. The FTIR pellets were each made from approximately 2 mg sample and 100 mg KBr.

The kinetic conversion from CEGx-MA to hydrogels during the UV curing process was analyzed by FTIR coupled with a single reflection diamond attenuated reflection (ATR) device. The UV source from a mercury lamp was directed to the sample using a fiber optic cable with an inner diameter of 1 cm. The intensity of the UV light, directed to the sample on the diamond crystal, was adjusted to 10 mW/cm^2 with a wavelength of 365 nm. The spectra were collected from hydrogels cross-linked at conversion time (t) up to 5 min. The conversion was calculated from integration of the decreasing peak area at 810 cm^{-1} (due to $-CH=CH_2$ vibration band of the methacrylic group) followed by normalization with the stretch vibration of $-CH_3$ at 2870 cm^{-1}, which remained unchanged during the course of the experiment. The conversion was calculated from the following equation

$$\text{conversion (\%)} = \left(1 - \frac{\frac{A_t}{B_t}}{\frac{A_0}{B_0}}\right) \times 100\%$$

where A_t and A_0 are the areas under the peak at 810 cm^{-1} at time t and time 0, respectively, whereas B_t and B_0 are the areas under the peak at 2870 cm^{-1} at time t and time 0, respectively.

Rheological behavior of CEGx-MA was performed with a Thermo Haake Rheostress 600 rheometer with a plate–plate geometry. One-hundred-fifty microliters of precursor solution was placed on the lower plate and the 2 cm diameter upper plate was lowered with a gap of 0.5 mm in between. The storage modulus (G′) and the loss modulus (G″), as a function of

temperature or time, were determined at an oscillation frequency of 1 Hz. Typically, the temperature was varied at the rate of 1 °C/min from 10 to 60 °C. For some samples, the cooling behavior was studied by cycling the temperature back from 60 to 10 °C at 1 °C/min.

The mechanical properties of both the physical and dual-cured hydrogels were characterized by compressive stress–strain measurements using an Instron 5543 Single Column Testing System with a 10 N-load cell. The physical gels were prepared according to the procedure as stated in sections 2.3 and 2.4 at 37 °C at various time durations (15 min, 25 min, 60 min and 24 h) and were immediately used for compression measurements. The dual-cured gels were prepared by 4-min UV irradiation of the physical gels formed at 25 min and 24 h and immediately used for the compression measurements. A cylindrical gel sample, 10 mm in diameter and 2 mm thick, was placed on the lower plate and compressed at a strain rate of 0.5 mm/min. The Young's modulus was calculated from the average slope of the stress–strain curve over the 0 to 20% strain range. The fracture stress and fracture strain were also reported. Three samples were tested for each gel preparation.

2.7. Cytocompatibility Tests. The primary SMCs used were from human aortic smooth muscle (Cambrex Bio Science Walkersville Inc.). SMCs were routinely maintained in tissue culture polystyrene flasks (TCPS) with growth medium (Dulbecco's modified Eagle's medium (DMEM) with 4 mM L-glutamine supplemented with 10% fetal bovine serum, 50 IU/mL of penicillin, and 50 mg/mL of streptomycin) (Gibco). Cells were passaged by trypsinization with 0.25% (w/v) trypsin and 0.03% (w/v) ethylenediaminetetraacetic acid (EDTA) solution (Sigma) before reaching confluence, usually every 4 days. Immediately after curing, the physical and dual-cured hydrogels were surface-grafted with RGD in 96-well cell culture dishes and then sterilized in 70% ethanol (30% DI H_2O) at room temperature for 24 h. Before cell seeding, the hydrogels CEG350-MA(-P and -D) and CEG2000-MA(-P and -D) were soaked with PBS for 1 h. SMCs and the culture medium were then added to the plate wells. The medium was changed every 2 days. At certain time points, phase contrast images were taken using a Zeiss inverted microscope. The seeding density was 1.0×10^5 cells/mL.

The primary human aortic endothelial cells (ECs) were obtained from Lonza Company (Lonza, Walkersville, MD). ECs were maintained in TCPS with Clonetics EGM–2 BulletKit (CC-3162) containing one 500 mL bottle of Endothelial Cell Basal Medium-2 and the following growth supplements: hydrocortisone, 0.2 mL; hFGF-B, 2 mL; VEGF, 0.5 mL; R3-IGF-1, 0.5 mL; ascorbic acid, 0.5 mL; heparin, 0.5 mL; FBS, 10 mL; hEGF, 0.5 mL; GA-1000, 0.5 mL (Lonza, Walkersville, MD). Cells were passaged by trypsinization with 0.25% (w/v) trypsin-0.03% (w/v) EDTA solution before reaching confluence, usually every 3 days. ECs were seeded on 96-well culture plate at the seeding density of 1.0×10^5 cells/cm^2.

Methyl tetrazolium (MTT) assay was used to examine mitochondrial function and cell proliferation. MTT solution with 5 mg/mL concentration was prepared by dissolving thiazolyl blue tetrazolium bromide in PBS. After cells were cultured for specified time periods, 100 μL MTT solution was added to the culture medium in each well of the 96-well plate containing hydrogels. The hydrogels were incubated on a shaker at 37 °C for 4 h for color development. The medium was removed after 4 h and DMSO was added to dissolve the formazan formed. The plate was incubated for another 2 h. After that, the DMSO with solubilized formazan was transferred to a 24-well assay plate and absorbance was measured using a microplate reader (Biorad) at a wavelength of 490 nm. Three parallels were averaged for each sample. The statistical significance between measurements on the two sets of data (CEG350-MA-P versus CEG350-MA-D, CEG350-MA-P versus CEG2000-MA-P, CEG350-MA-D versus CEG2000-MA-D and CEG2000-MA-P versus CEG2000-
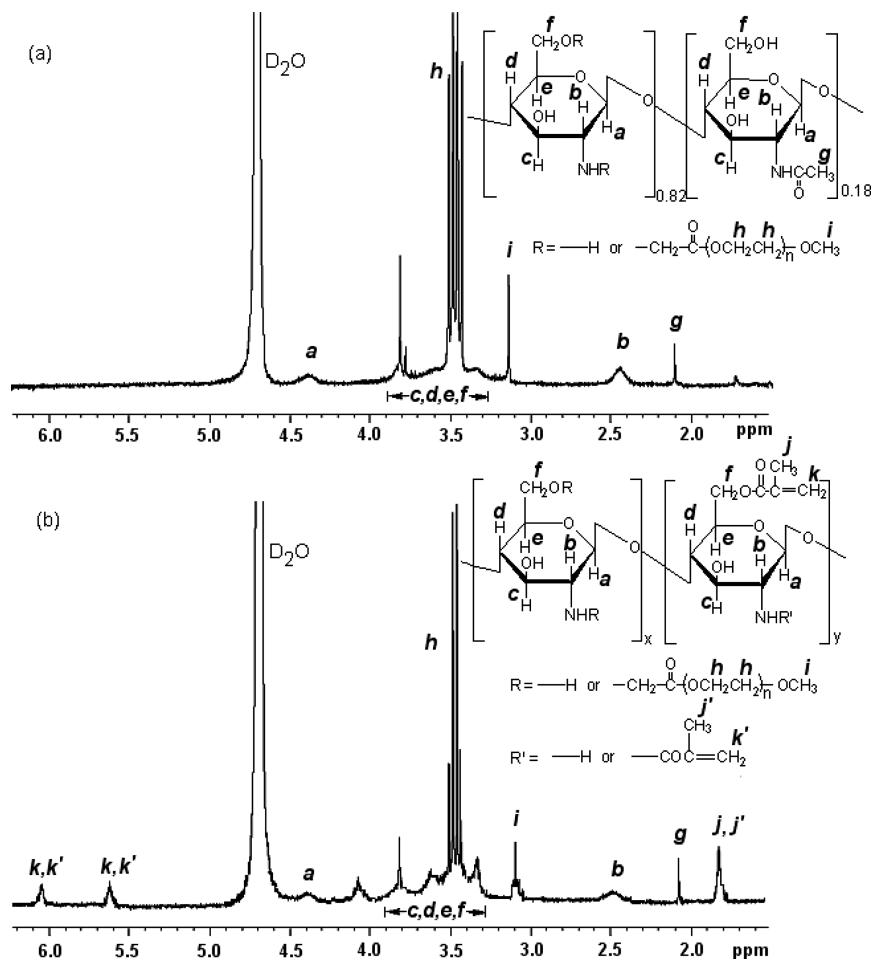
FIGURE 1. ^{1}H NMR spectra of (a) CEG350, and (b) CEG350-MA in D$_2$O (300 MHz).

MA-D comparisons) was calculated using Student's *t* test. Differences were taken to be significant when a *p*-value of 0.05 or less was obtained (showing a 95% or higher confidence limit).

2.8. Layer-by-Layer (LBL) Cell Culture. Cells at the density of 1.0×10^5 (cells/mL) were deposited on TCPS and grown for 2.5 days to confluence, after which the medium was pipetted from the wells. Gel solution (5 wt % CEG350-MA and 95% autoclaved PBS) was then added to the wells (50 μL/well). The CEG350-MA solutions were then incubated in an incubator for 25 min to physically gel. Two-hundred microliters of culture medium was then added for 2 h. A second layer of cells was then seeded. When they had adhered (about 4 h), the experiments were separated into 3 groups (Scheme 1): (a) Control, the precursor gel solution was applied to the second cell layer and the assembly incubated at 37 °C for 25 min for physical gelation. The cells were then cultured for 2 days. (b) UV before confluence: the precursor gel solution was applied to the second cell layer and the assembly incubated at 37 °C for 25 min to allow physical gelation and then UV irradiated for 4 min. The cells were then cultured for 2 days before observation. (c) Delayed UV, the cells were cultured for 2 days before the precursor gel solution was added. The solution was incubated at 37 °C for 25 min and UV-irradiated for 4 min. After an additional 2 days of culture, the cells were observed. The second layer of cells was cultured for 2 days unless otherwise specified. For all three experimental conditions, live/dead analyses were performed to observe the viability of the cells.

Live/dead assay for cell viability was applied to determine the cell viability for the LBL cell culture. One-hundred-fifty microliters of combined LIVE/DEAD assay reagents (4 μL of 2 Mm EthD-1 stock solution and 1 μL of 4 Mm calcein AM stock solution in 2 mL PBS) were added to each well of the cell culture dish. The cells were incubated for 30 min. After incubation, 100 μL of PBS was added to each well and then the labeled cells were observed with fluorescence microscopy.

3. RESULTS

3.1. Synthesis and Characterization of CEGx and CEGx-MA. Scheme 2b shows the reaction procedure to obtain CEGx and CEGx-MA. Chitosan was first deprotonated, before adding chlorofunctionalized-PEG, by reaction with NaOH. Because NaOH is a strong base, both the amine (at C2 position) and the primary alcohol (at C6 position) present in chitosan could be deprotonated, and the PEG was subsequently grafted at both the amine and the primary alcohol, to produce CEGx. CEGx was then methacrylated in a tranesterification reaction to form CEGx-MA using glycidyl methacrylate and triethylamine as base. Similarly, both the amine and the alcohol of chitosan could be methacrylated. Reactivity at the secondary alcohol at C3 position is probably poor for both reactions since the C3-OH might be engaged in hydrogen bonding (39), rendering it less reactive than the primary alcohol at the C6 position (40).

^{1}H NMR was carried out to characterize CEGx and CEGx-MA. Representative ^{1}H NMR spectra of CEG350 and CEG350-MA are shown in Figure 1. The resonance signal at 3.5 ppm
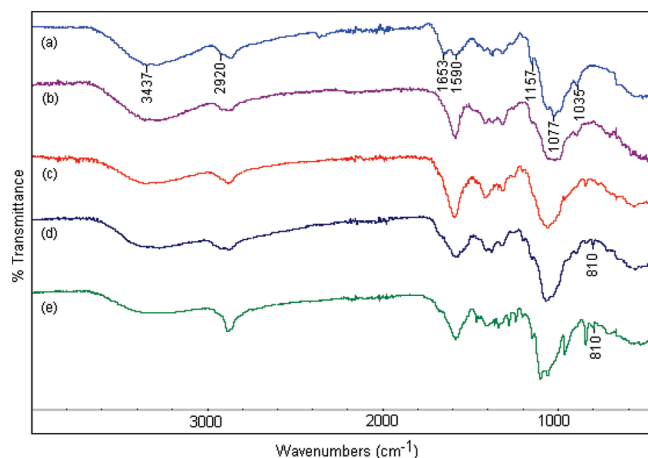
FIGURE 2. FTIR spectra of (a) chitosan, (b) CEG350, (c) CEG2000, (d) CEG350-MA, and (e) CEG2000-MA.

Table 1. Chemical Analysis and Solubility of Chitosan, CEGx, and CEGx-MA

	after PEGylation		
	chitosan	CEG350	CEG2000
yield (%)		61.9	30.3
DS by PEG (mol %)		16.0 ± 0.1	29.0 ± 0.1
NH_2 (mol %)	48.4 ± 4.3	35.5 ± 1.3	21.2 ± 2.7

	after methacrylation		
	chitosan	CEG350-MA	CEG2000-MA
water solubility	insoluble	soluble	soluble
NH_2 (mol %)	48.4 ± 4.3	11.6 ± 0.1	8.3 ± 1.8
DS by methacrylate group (mol %)		21.6 ± 0.7	20.2 ± 0.4

(*h*) in the spectrum of CEG350 is attributed to the methylene protons in PEG while the 3.2 ppm (*i*) signal is due to the protons of the terminal $-CH_3$ group of PEG (41). These resonance signals of PEG methylene protons overlapped with some of the signals present in the chitosan backbone (labeled as *c, d, e, f* in Figure 1). The signal at 2.1 ppm (*g*) is attributed to -NHCOCH_3 on chitosan. After methacrylation to produce CEG350-MA, resonance signals attributed to protons and methyl group attached to the double bond were observed at 5.6 and 6.1 ppm (*k, k'*) and 1.9 ppm (*j, j'*), respectively (Figure 1b).

FTIR spectra of vacuum-dried chitosan, CEG350, CEG2000, CEG350-MA, and CEG2000-MA are shown in Figure 2. Figure 2a shows the characteristic absorbance features of the native chitosan molecule: 3437 cm^{-1} (O−H stretch), 2920 cm^{-1} (sp^3 C−H vibration), 1653 cm^{-1} (amide I band, C−O stretch of acetyl group), 1590 cm^{-1} (N−H bend), 1157 cm^{-1} (bridge-O-stretch), 1077 cm^{-1} (C−O stretch), and 1035 cm^{-1} (C−O stretch). In the FTIR spectra of CEG350 and CEG2000 (Figure 2b,c), the 1077 cm^{-1} C−O stretch of chitosan overlapped with the C−O stretching band of PEG (∼1070 cm^{-1}) (41) so that the peak at 1077 cm^{-1} is relatively broad. The absorbance bands at 3400 cm^{-1} and 1157 cm^{-1} (Figure 2b,c) which are characteristic of OH group and 6-OH of chitosan have reduced in intensity for CEG350 and CEG2000, inferring that PEG substitution has occurred at the OH position (38, 42, 43). For the FTIR spectra of CEG350-MA and CEG2000-MA (Figure 2d,e), the formation of a new peak at around 810 cm^{-1} is attributed to the vinyl bond of the terminal methacrylate group (44); the slight reduction in intensity of absorbance at 3400 cm^{-1} (OH stretching) relative to CEGx inferred that methacrylation has also occurred at the OH group (42, 43). FTIR suggested that both the PEGylation and methacrylation can occur at the 2-N and 6-OH positions.

3.2. Physical Properties of CEGx and CEGx-MA.

Some physical characteristics of CEG350 and CEG2000 are summarized in Table 1. The degree of PEG substitution in CEG350 and CEG2000 are 16.0 ± 0.1 mol % and 29.0 ± 0.1 mol % respectively. The higher amount of grafted PEG present in CEG2000 is due to the longer reaction time

needed to increase the reaction yield. The lower reaction yield of CEG2000 was caused by steric hindrance of the longer PEG chain. At the ambient reaction temperature, 1 day was required to achieve 62% yield for CEG350, whereas CEG2000 had to be reacted for 2 days to achieve a yield of 30%. From the ninhydrin analysis (36, 37), the NH_2 (mole %) content of CEG350 and CEG2000 were measured to be $35.5 \pm 1.3\%$ and $21.2 \pm 2.7\%$, whereas that of native chitosan is $48.4 \pm 4.3\%$ (Table 1). Some of the amine functionality in chitosan was replaced with PEG.

After methacrylation, the NH_2 content decreased to $11.6 \pm 0.1\%$ and $8.3 \pm 1.8\%$ for CEG350-MA and CEG2000-MA, respectively, indicating that amino groups were further substituted by the methacrylate group. Through elemental analyses, CEG350-MA and CEG-2000-MA were found to have degrees of methacrylation of 21.6 ± 0.7 and 20.2 ± 0.4 mol %, respectively (Table 1). Unlike pristine chitosan, both CEG350-MA and CEG2000-MA are soluble in water at physiological pH.

Figure 3a shows the FTIR spectrum of CEG350-MA at different photo-cross-linking times up to 5 min. The peak at around 810 cm^{-1} has almost disappeared at 4 min and a hydrogel film that could be handled with ease was produced at this point. Figure 3b shows the methacrylate conversion versus UV exposure time for CEGx-MA. After 4 min of UV exposure, CEG350-MA and CEG2000-MA were 86 and 88% converted, respectively. CEG2000-MA has a faster conversion compared to CEG350-MA, probably because of the methacrylate being on a longer chain of PEG, which allows for greater mobility of unsaturated bond during the photo-polymerization reaction.

3.3. Hydrogel Physical Properties.

Dynamic rheological experiments were performed as a function of temperature (Figure 4a−c,e) and time (Figure 4d) for 5 wt % solutions of CEG350-MA and CEG2000-MA. Figure 4e shows the hysteresis study of CEG350-MA. Panels a and b in Figure 4 show that both G′ and G″ are low in the solution state, but G″ is larger than G′ below the crossover point, which is typical of liquids (27, 30). Both G′ and G″ increase gradually until about 37 °C, when crossover occurs. The crossover temperature is the gelation temperature at which sol/gel transition occurs. After gelation, G′ is larger than G″ for both gels, indicative of elastic solids (27, 30), and both
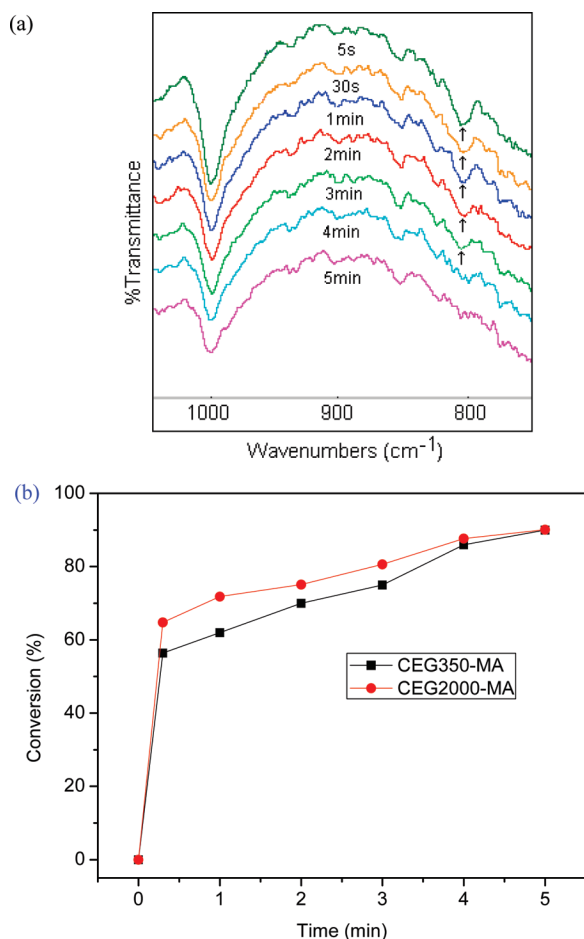
(a)

(b)

FIGURE 3. (a) FTIR spectra of CEG350-MA cured at different photo-cross-linking time and (b) photocuring conversion of CEGx-MA.

G' and G'' increase dramatically. For CEG350-MA-P, G' and G'' increase dramatically from 1.2×10^1 Pa to 1.3×10^5 Pa and 3.1×10^1 Pa to 7.1×10^4 Pa, respectively, at about 50 °C, whereas for CEG2000-MA-P, G' and G'' increase from 1.8×10^1 Pa to 3.3×10^4 Pa and 2.4×10^1 Pa to 5.1×10^3 Pa, respectively. Warming CEG350-MA and CEG2000-MA solutions causes gelation at about 37 °C and increases G' and G'' by 4−5 and 3−4 orders of magnitude, respectively. CEG350-MA-P is the stiffer of the two gels.

Figure 4c shows that starting at around 37 °C and ending in the mid 50 °C, there is a rapid increase in viscosity from 6.0 to 4.0×10^5 Pa s and from 3.6 to 1.2×10^3 Pa s for CEG350-MA and CEG2000-MA, respectively. Figure 4d shows the time dependence of G' for the gels at 37 °C: it indicates that G' for CEG350-MA and CEG2000-MA increase with time and eventually reach a plateau of about 2×10^5 Pa after 20−25 min, at which point gelation is complete (33).

Figure 4e shows the rheological behavior of a CEG350-MA solution during a heating−cooling cycle from 10 to 60 °C and back to 10 °C. The sharp increase in G' upon heating indicates that the liquid solution could turn into a solid-like gel at around 37 °C and the decrease in G' during cooling shows that the gel tended to revert back to a liquid at a lower temperature of about 25 °C, though G' does not return to the initial value. By visual observation, the physical gel

became a viscous liquid with some sol forming upon cooling, though some gel still remained after cooling.

Compression tests were carried out at room temperature (Figure 5). The physical gels at the onset of formation were very soft but the elastic modulus and ultimate stress increased significantly with 24 h incubation at 37 °C; for incubation from 15 to 60 min, the Young's modulus and fracture stress were not significantly different. It seems that substantially longer than 60 min (e.g., 24 h) of physical gelation is necessary for significant increase of the compressive properties. For CEG350-MA-P, the elastic modulus and ultimate stress increased from 1.5 ± 1.2 kPa and 2.1 ± 1.8 kPa at 15 min to 19.5 ± 4.0 kPa and 7.2 ± 2.7 kPa after 24 h respectively (Table S1 in the Supporting Information). For CEG2000-MA-P, the elastic modulus and ultimate stress increased from 0.8 ± 0.6 and 0.7 ± 0.8 kPa after 15 min to 24.7 ± 8.7 and 9.1 ± 2.5 kPa after 24 h, respectively. The 24 h fracture moduli of CEG350-MA-P and CEG2000-MA-P were not significantly different.

UV irradiation further increased the moduli of dual-cured hydrogels (with 25 min and 24 h physical gelation) modestly to 2−3 times that of the corresponding physically cured hydrogels.

3.4. Biological Properties of CEGx-MA Hydrogels. SMCs were cultured on physically gelled and dual-cured CEG350-MA and CEG2000-MA (Figure 6). Comparing the four hydrogels, it appears that the CEG350-MA series (both physically gelled and dual-cured, i.e., CEG350-MA-P and CEG350-MA-D) supports cell spread and proliferation better than the CEG2000-MA series (i.e., CEG2000-MA-P and CEG2000-MA-D). For the CEG350-MA series, cells were well spread out and spindle-shaped, whereas cells on the CEG2000-MA series remained round. The MTT results (Figure 7) also confirmed that compared to the CEG2000-MA series, the CEG350-MA series had significantly more viable cells though fewer than TCPS. The viable cell numbers for the CEG350-MA series increased with culture time, indicating the biocompatibility of this series (Figure 7). Further, the dual-cured CEG350-MA-D hydrogel appeared to support better cell proliferation and growth than the CEG350-MA-P hydrogel. This may be due to the higher stiffness of the dual-cured hydrogel.

CEG350-MA was used for LBL cell culture using SMCs (Scheme 1). The first layer of cells was grown on TCPS to confluence and then CEG350-MA solution was deposited on the confluent layer and allowed to physically gel. The thickness of each gel layer was approximately 200 μm (see Figure S1 in Supporting Information) as observed by optical microscopy. Then a second layer of SMCs was seeded on the first layer of CEG350-MA-P gel and the samples were divided into three groups. In culture condition "a" (Scheme 1, setup 5a), more CEG350-MA solution was dispensed and the second layer of cells was encapsulated in the second layer of CEG350-MA-P hydrogel. The cells were then cultured for 2 days and then stained for the live/dead assay. Virtually no dead cells were detected in setup 5a (Scheme 1), in which the cells were not exposed to UV irradiation (Figure 8a). This
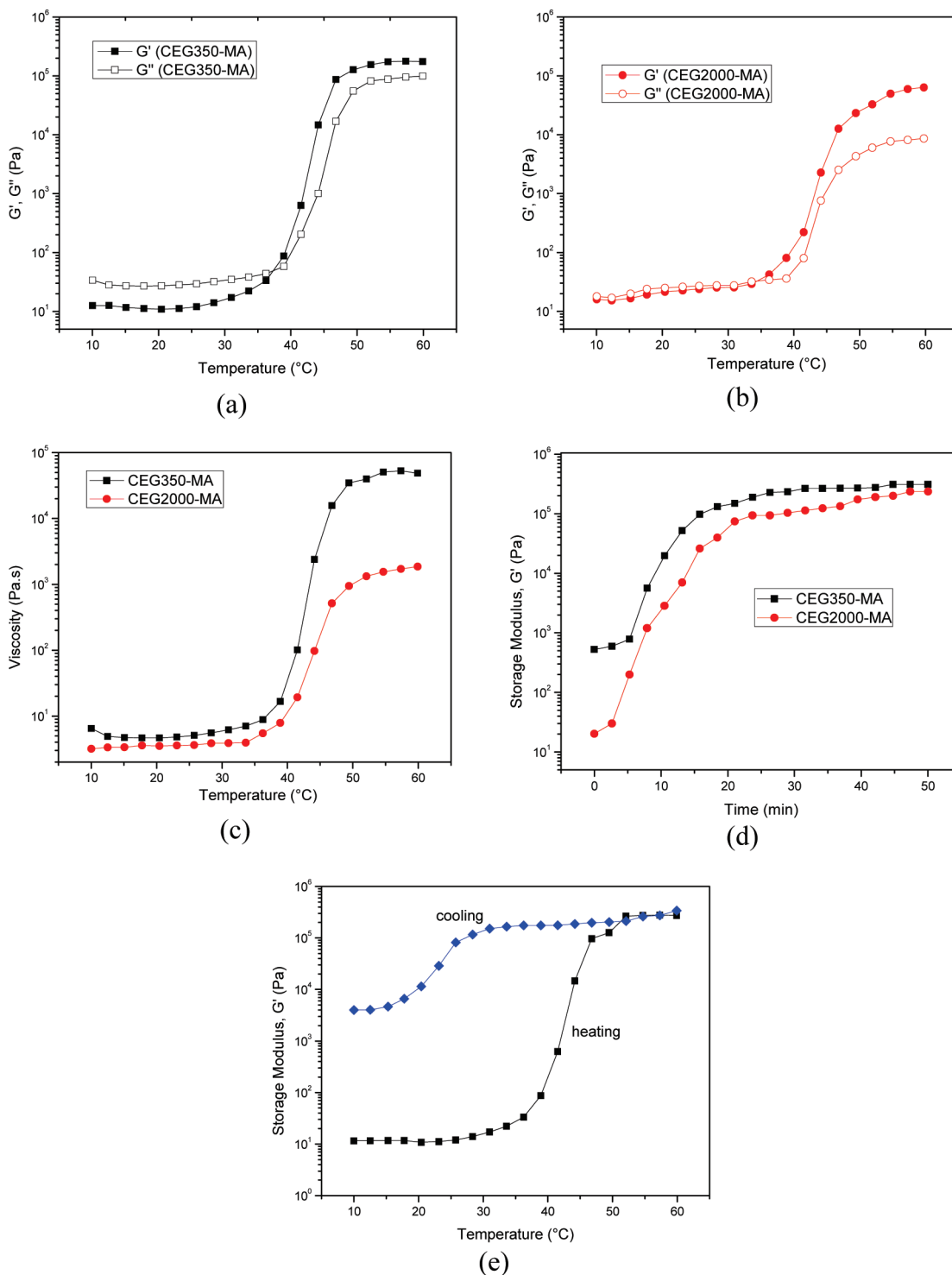
FIGURE 4. Rheological analysis of CEGx-MA with 5% polymer precursor. Temperature dependence of G′ and G″ for (a) CEG350-MA and (b) CEG2000-MA. (c) Temperature dependence of viscosity. (d) Time dependence of G′ at 37 °C. (e) Sol−gel transition of CEG350-MA during a heating−cooling cycle between 10 and 60 °C.

indicates that the CEG350-MA-P hydrogel is biocompatible. In condition "b" (setup 5b), CEG350-MA solution was dispensed onto the second layer of cells, physically gelled for 25 min and then UV-irradiated for 4 min. The cells, encapsulated inside the dual-cured CEG350-MA-D gel, were cultured for 2 days before the live/dead analysis. A few more dead cells were observed via optical microscopy in setup 5b

than in setup 5a (Figure 8b). The dead cells were possibly due to UV exposure or the higher gel stiffness. In condition "c" (setup 5c), we cultured the second layer of cells to confluence for 2 days before adding CEG350-MA solution, which was then hardened by physical gelation for 25 min and UV irradiation for 4 min. More dead cells were observed in setup 5c than in setups 5a or 5b (Figure 8c). Figure 8

(a)

(b)
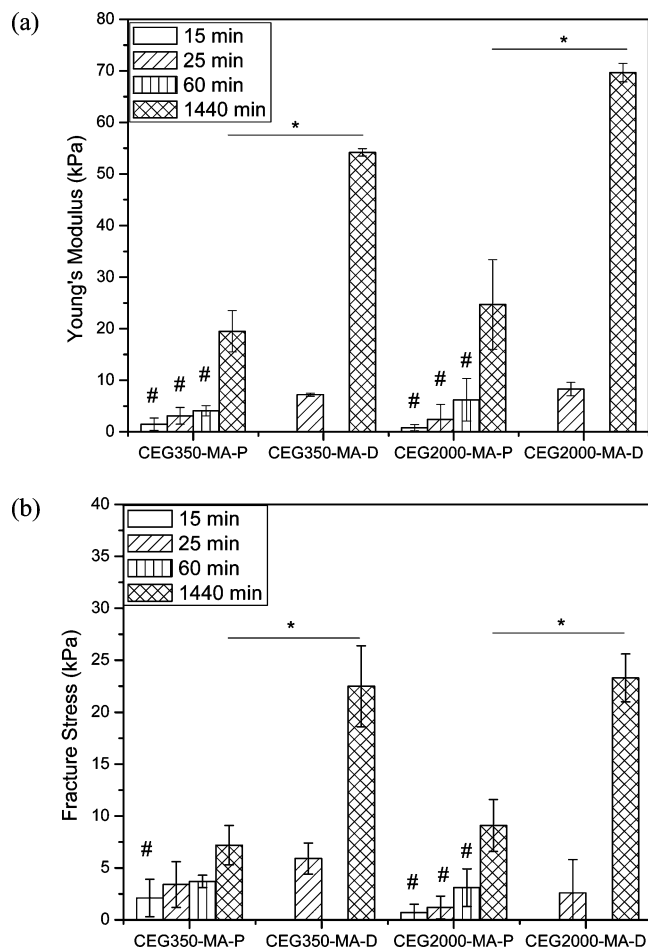
FIGURE 5. (a) Young's modulus and (b) fracture stress with respect to physical gelation time for CEGx-MA-P and CEGx-MA-D (at the level of $P < 0.05$, * significantly different from that of CEGx-MA-D at 1440 min; # significantly different from that of CEGx-MA-P at 1440 min gelation time).

shows that SMCs can generally grow well in the gels in all three setups, although more dead cells were found in setup 5c.

The effects of gel thickness and different cell types cultured in the LBL setup were also investigated. Gel thicknesses of about $150-280\,\mu m$ were produced by varying the volumes of gel solution added ($25-75\,\mu L$); addition of 25, 50, and $75\,\mu L$ of gel solutions resulted in gel thicknesses of about 150, 200, and $280\,\mu m$, respectively. Figure 9 shows that the number of dead cells increases with increasing gel thickness. To investigate the culture of different types of cells, ECs and SMCs were cultured in one setup, with ECs as the first cellular layer and a hydrogel layer between this layer and the next cellular layer of SMCs. Figure 10 shows that cells in the ECs/CEG350-MA/SMCs/CEG350-MA layered constructs are mostly alive even in the presence of UV.

4. DISCUSSION

Pristine chitosan is soluble only at acidic pH due to the presence of $-NH_2$ and $-OH$ leading to strong hydrogen bonding. Grafting of PEG chains decreases the hydrogen bonding leading to the collapse of the crystalline structure of chitosan so that chitosan-*graft*-PEG is soluble in neutral pH (42). PEG is a highly hydrated molecule with a high

exclusion volume due to the attraction of many water molecules, which reduces its interaction with other molecules. Though methacrylation increases the hydrophobicity, CEGx-MA copolymers were found to still be water-soluble at physiological pH so that cell encapsulation with these hydrogels was feasible.

Bhattarai et al. (31, 32) have shown that chitosan-*graft*-PEG is a thermoresponsive hydrogel and found that it gels at 37 °C. At low temperature, there is strong intermolecular hydrogen bonding between water and PEG. As the temperature is raised, interaction of PEG with water is decreased so that hydrogen bonding is reduced. Hydrophobic interactions between chitosan backbone and/or methylene groups in PEG become stronger, compared to hydrogen bonding, so that gel formation occurs (31, 32). Both CEG350-MA and CEG2000-MA can form physical hydrogels at around 37 °C and their G′ increase impressively by 4−5 orders of magnitude to become elastic solids at 37 °C and higher temperatures. We observed that higher polymer concentration and slower temperature ramping rate would increase the final G′ of the solidified gel. Rheology experiments also show that the physical gels are somewhat thermoreversible (Figure 4e).

The rheology measurements (Figure 4a and b) indicate that CEG2000-MA-P gel has lower dynamic elastic modulus than CEG350-MA-P. This could be attributed to the longer characteristic time for PEG2000 folding and rearrangement, leading to a weaker physical gel before equilibrium. However, both eventually attain almost the same G′ when held at 37 °C (Figure 4d), which corroborates with the compressive modulus results which show insignificant difference between CEG350-MA-P and CEG2000-MA-P gelled under the same conditions (Figure 5).

The stiffness increase with further UV irradiation depends somewhat on the physical gelation period applied. For example, after 25 min of physical gelation, UV cross-linking of CEG350-MA-P to form CEG350-MA-D increased stiffness by 130%, whereas after 24 h of gelation, the UV-induced stiffness increase was 180%. However, the compressive strength and modulus increase caused by the 4 min of UV irradiation is small compared to the increase with longer physical gelation time (6−10 times increase with 24 h standing). This could be attributed to the steric hindrance experienced by the methacrylate group during UV irradiation. The short UV irradiation time (4 min) was chosen to minimize UV damage to encapsulated cells while somewhat improving the gel mechanical properties and, most importantly, making them thermally stable. Both polymers were also more than 80% converted at this point (Figure 3). A longer physical gelation time (e.g., 24 h) is necessary for significant increase of the compressive properties (Figure 5). After UV cross-linking, the gel is not reversible back to the sol, unlike the physical gel shown in Figure 4e. A more thermally stable gel is preferable for tissue culture, handling and implantation.

Cell processes can be influenced by both mechanical and chemical properties of the substrate. It has been shown that gel stiffness plays an important role in cell processes.
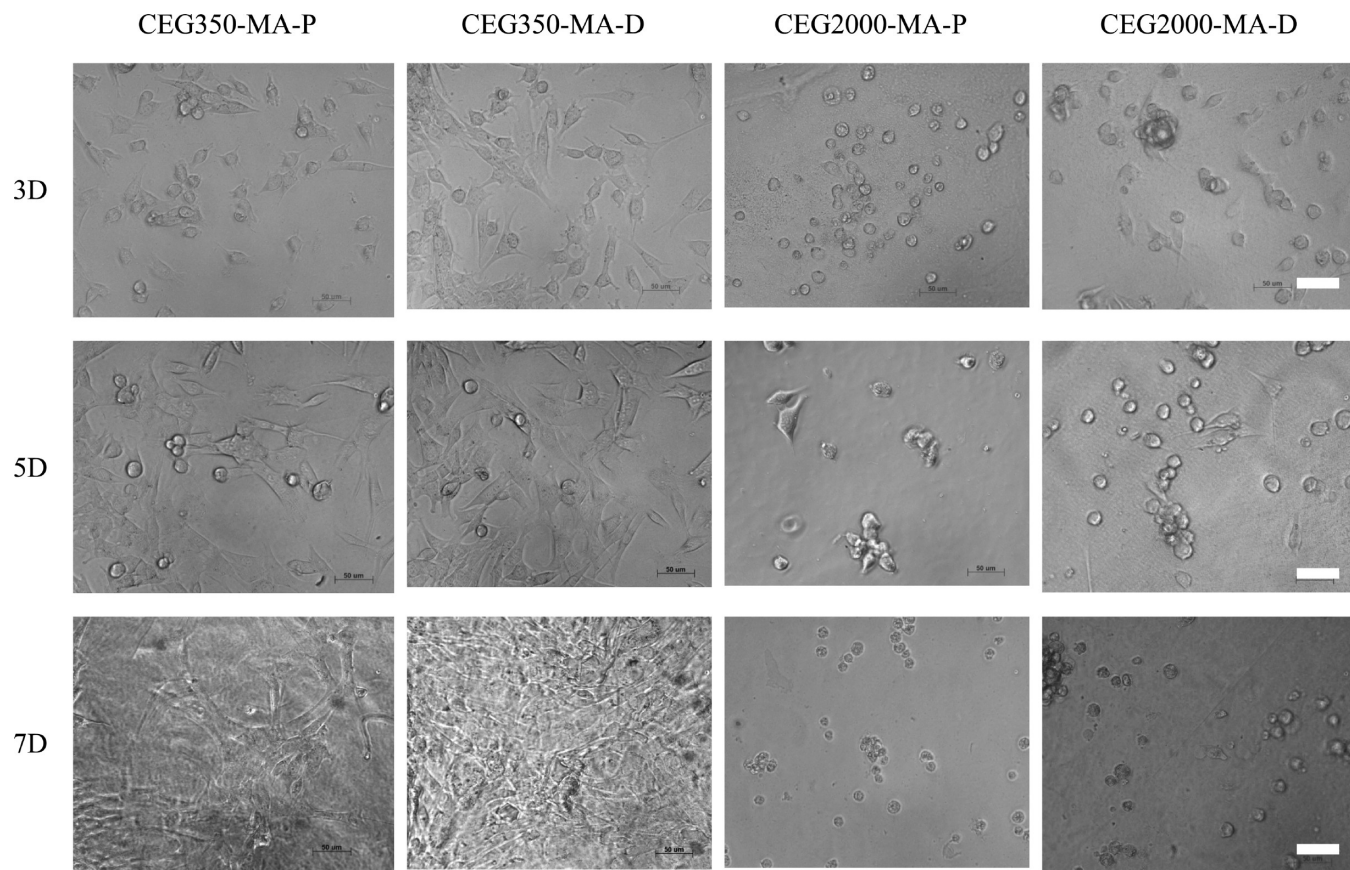
CEG350-MA-P   CEG350-MA-D   CEG2000-MA-P   CEG2000-MA-D

FIGURE 6. Cell morphology on RGD-grafted physical gels (CEG350-MA-P and CEG2000-MA-P) and RGD-grafted dual-cured hydrogels (CEG350-MA-D and CEG2000-MA-D) at different periods of cell culture (scale bar = 50 μm). Physical gels were made by 25 min incubation at 37 °C.
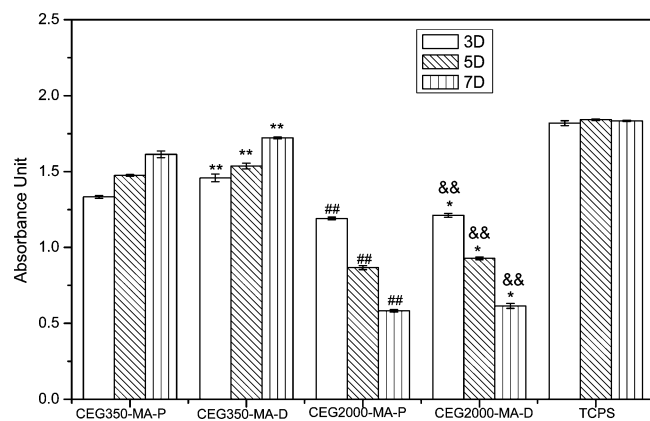

FIGURE 7. MTT activities (absorbance at 490 nm) of cells cultured on RGD-grafted CEGx-MA hydrogels for up to 7 days. Error bars represent mean ± standard deviation for $n = 3$. The seeding density was 1×10^5 cells/mL (at the level of $P < 0.001$, ** significantly different from that of CEG350-MA-P hydrogel at the same day of culture, ## significantly different from that of CEG350-MA-P hydrogel at the same day of culture, && significantly different from that of CEG350-MA-D hydrogel at the same day of culture; at the level of $P < 0.05$, * significantly different from that of CEG2000-MA-P hydrogel at the same day of culture).

Variation in matrix stiffness is known to cause different focal adhesion structure, cytoskeleton organization, cell morphology, and protein expression (45–47). To study the influence of gel stiffness and chemical structure on biocompatibility of these hydrogels, 2D cell culture was carried out with CEGx-MA-P and CEGx-MA-D. The physical gels were made

by incubating 5 wt % polymer solution at 37 °C for 25 min; some of the physical gels formed were further UV irradiated for 4 min to form dual-cured gels. All the gels were surface-grafted with RGD prior to cell seeding. RGD grafting was done after the gel formations step(s) to avoid modulation of the thermoresponsive behavior of the gel precursor. Although cells do not grow well on CEGx-MA-P and CEGx-MA-D without RGD, grafting with RGD significantly improves the cytocompatibility of these hydrogels. On the basis of the cell morphology and MTT results, the CEG350-MA series (both -P and -D) supports cell spreading and proliferation better than the CEG2000-MA series. Although the two series have similar mechanical properties, the CEG350-MA series is more hydrophobic because the PEG chain is shorter and the PEG content is lower than in the CEG2000-MA series, which may account for its better biocompatibility (48–50). Also, comparing CEG350-MA-P and CEG350-MA-D, the dual-cured gel has significantly higher cell spread and proliferation, which may be due to its higher modulus (Figure 7, $P < 0.001$).

Figure 8 shows that our hydrogel can be used to build up two cell layers by the LBL technique. The left column shows the results with 2-day culture for the second layer of cells. Cells encapsulated inside the first layer of CEG350-MA-P hydrogel are mostly alive. The first layer of cells would secrete some multiadhesive proteins such as collagen so that the second layer of cells generally grows well in the three setups. There were more dead cells in setup 5c (Figure 8ci),
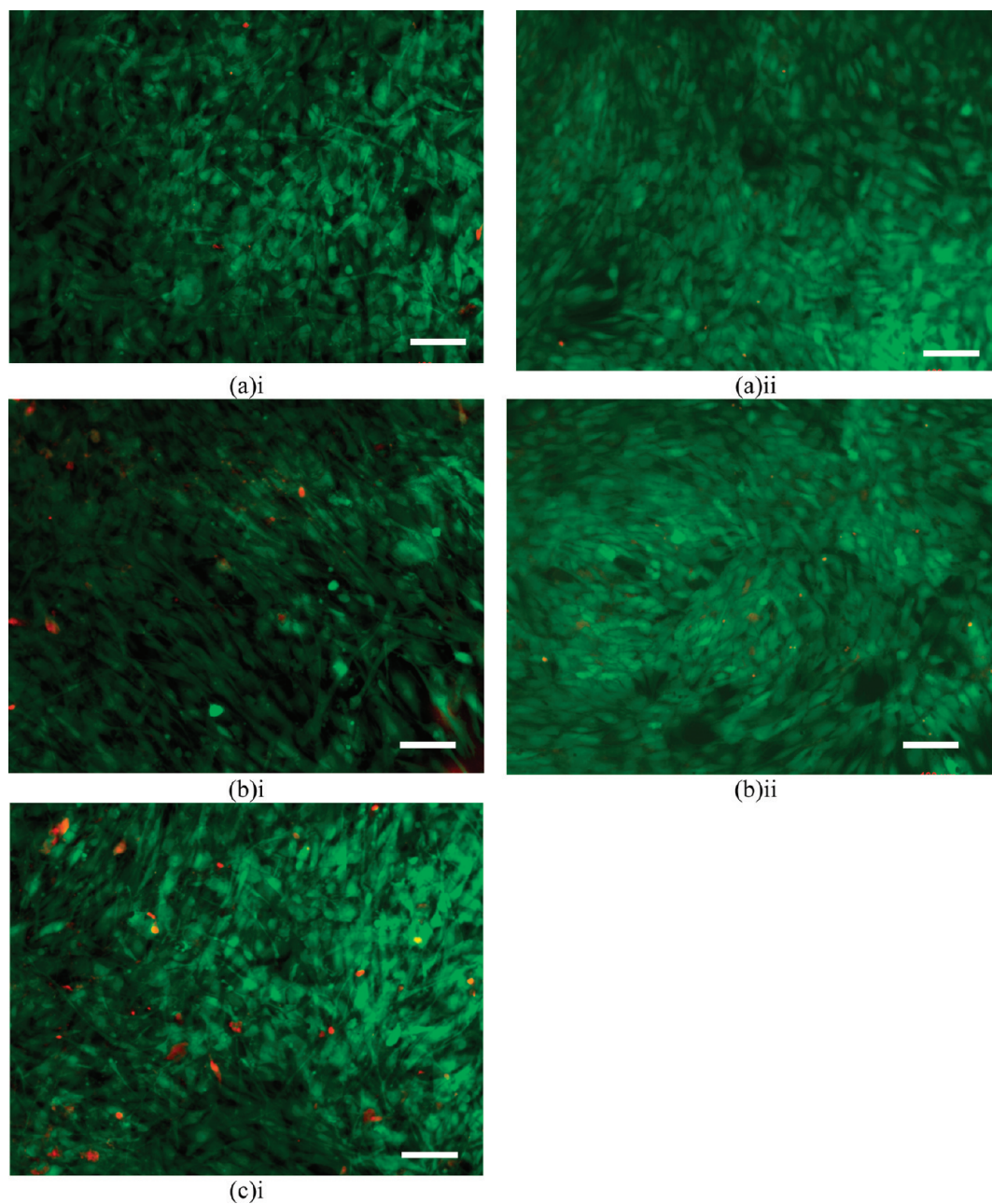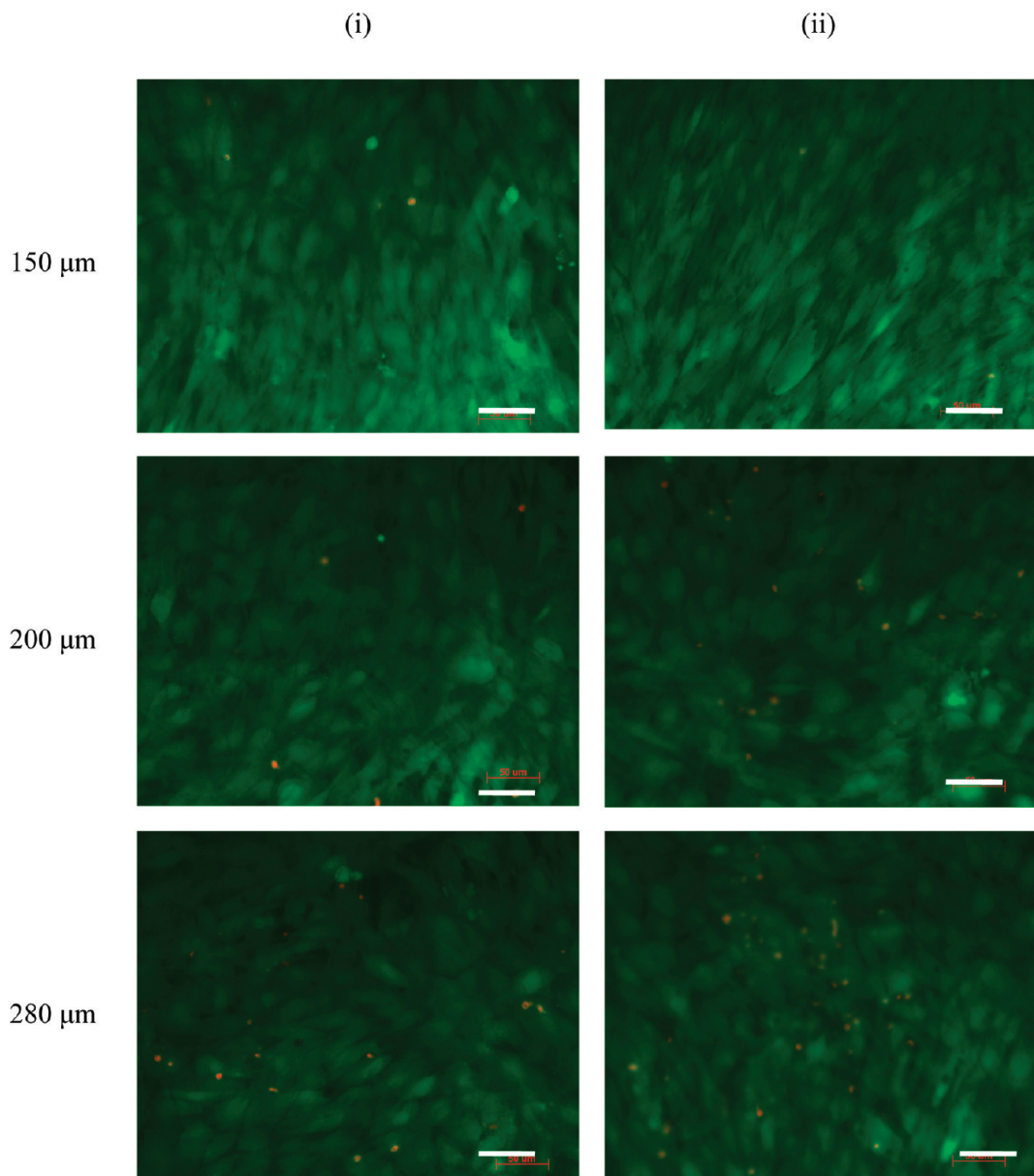
FIGURE 8. Inverted fluorescence microscopy of live/dead test for different LBL conditions of SMC culture with CEG350-MA gels as shown in Scheme 1. 2nd layer of cell is cultured for (i) 2 days or (ii) 14 days. (a) Control group with two layers of gel and no UV (setup 5a). (b) UV group setup with gels exposed to UV immediately after deposition of second layer of cells (setup 5b). (c) Delayed UV group- setup with gels exposed to UV after two days of proliferation of the second cell layer (setup 5c).

which has more cells because the second layer of cells was allowed to be confluent. (However, there were also more live cells in setup 5c). It is not obvious that the ratio of dead cells to total cell number in setup 5c has substantially increased over that of setup 5b (Figure 8bi). In setup 5ai with physical gelation only, the number and fraction of dead cells is small. The increase in dead cells in 5bi and ci over ai is plausibly attributed to the UV irradiation of bi and ci, whereas the increase in ci over bi may simply be due to the larger total number of cells in c, with two confluent layers.

In addition, the second layer of cells was allowed to grow for 14 days in setup 5a and 5b; Figure 8aii and bii shows that cell viability was not affected with longer culture.

Nutrients were replenished with fresh culture medium every 2 days and these were absorbed by the hydrogels; the absorbed nutrients together with collagen secreted by cells enable the SMCs to survive for prolonged times. Dissolution of the scaffold over this period was not determined in the cell culture condition, but it is believed that some part of the gels might be replaced by ECM (though the gel is still visible after 14 days), which in a way also supports the survival of the cells.

Figure 9 shows that a thicker gel layer would result in more dead cells (though there are still a majority of live cells), this is probably attributed to an increased barrier to the diffusion process of nutrients secreted by the first layer of

(i) (ii)

FIGURE 9. Inverted fluorescence microscopy of live/dead test for SMCs culture for different thickness of CEG350-MA gels in the LBL setup. 2nd layer of cells was cultured for 2 days. (i) Control group with two layers of gel and no UV (setup 5a, scheme 1). (ii) UV group setup with gels exposed to UV immediately after deposition of second layer of cells (setup 5b, Scheme 1). Scale bar = 50 μm.

cells and nutrients from the culture medium to reach the other layer of cells (51). However, a thin gel would usually break during rinsing and changing of medium, hence, a gel thickness of 200 μm was selected here to achieve good cell viability and eliminate the rinsing problem.

The LBL process can be extended to more than two layers by successive implementation of steps 3 and 4 of Scheme 1, with a culture period to allow the new cell layer to become confluent before the next gel layer is added. Figure 8 suggests that the ratio of dead to live cells in each layer of a multilayer construct would be low, so that a thick tissue with predominantly live cells could be constructed with multiple LBL steps. The construct would finally be UV irradiated as in setup 5b (Scheme 1) to make it thermally stable. This approach minimizes UV damage to the cells in the construct. A multilayer construct made with a conventional UV-only

curing gel precursor would require repeated UV irradiation of the construct to gel each successive layer, which would limit the achievable tissue thickness or destroy many of the cells in the construct. With a thermoresponsive and also UV curable gel precursor, such as CEG350-MA, a thick tissue may be built up with the LBL technique in which each layer is non-cell-destructively gelled thermally and the final thick construct is rendered thermally stable for handling and use with a single UV exposure.

Successive buildup of alternate layers of SMCs and gels would produce stratified structures that more closely mimic the layered architecture of biological tissues and organs, such as blood vessels. CEG350-MA gel provides a controllable and versatile synthetic matrix alternative to collagen gel that has been used to build layered cellular construct (52); CEG350-MA is also water-soluble and nontoxic and exhibits unique
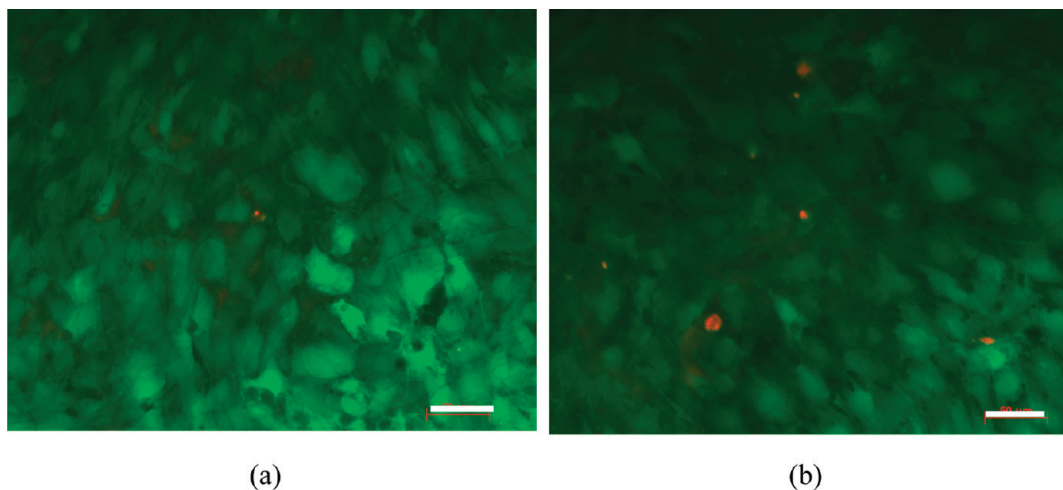
FIGURE 10. Inverted fluorescence microscopy of live/dead test for EC and SMC culture with CEG350-MA gels and ECs as the first layer of cells in the LBL setup. (a) Control group with two layers of gel and no UV (setup 5a, Scheme 1). (b) UV group setup with gels exposed to UV immediately after deposition of second layer of cells (setup 5b, Scheme 1). Scale bar = 50 μm.

thermogelling properties. We have shown that SMCs/CEG350-MA/SMCs/CEG350-MA constructs could be built up with controlled thickness. In order to better mimic vascular tissue where SMCs layer is lined with ECs, these two cell types were cultured in one setup. Figure 10 shows that the ECs and SMCs in the ECs/CEG350-MA/SMCs/CEG350-MA layered constructs could grow well whether in the absence or presence of UV. The current setup can thus be potentially applied as a scaffold to study different cellular responses to a variety of biological cues.

5. CONCLUSIONS

We have synthesized two chitosan-*graft*-PEG-*graft*-methacrylate (CEGx-MA) copolymers with PEG molecular weights (M_n) of 350 and 2000 Da. CEG350-MA and CEG2000-MA are both water-soluble and their solutions (5 wt %) undergo gelation to form hydrogels when the temperature is raised to about 37 °C. The mechanical properties significantly improve as the gels are maintained at the gelation temperature (37 °C) for 24 h. UV irradiation further increases the modulus of dual-cured hydrogels 2- to 3-fold and forms thermally stable dual-cured networks. The modulus of CEG350-MA-P and CEG350-MA-D after 24 h/37 °C incubation were 19.5 ± 4.0 and 54.2 ± 0.7 kPa, respectively; the corresponding ultimate strength of CEG350-MA-P and CEG350-MA-D after incubation were 7.2 ± 2.7 and 22.5 ± 5.9 kPa, respectively.

The CEG350-MA series is more biocompatible than the CEG2000-MA series; within the CEG350-MA series, the dual-cured CEG350-MA-D exhibits better biocompatibility with SMCs than the physically gelled CEG350-MA-P. LBL cell culture with CEG350-MA was successfully performed to build up two layers of cell/hydrogel construct. The CEG350-MA solution and gel were both nontoxic to the cells. Cells remained mostly viable when encapsulated inside CEG350-MA-P and CEG350-MA-D hydrogels, though some dead cells were seen with the latter. Layer-by-layer culture is an attractive approach to the rapid formation of thick tissues. Our thermoresponsive hydrogels illustrate the possibility of build-

ing thick tissues by the LBL technique. The ability of these materials to gel without UV irradiation of each layer should improve the health of thick synthetic tissues while the material can be made thermally stable and somewhat stronger by a single UV exposure after thick tissue buildup is complete. These materials, or materials with their properties, should be highly useful in tissue engineering.

Supporting Information Available: Table of compressive properties of hydrogels at room temperature; photographs of hydrogel layer showing the thickness along different sections of the gel. These materials are available free of charge via the Internet at http://pubs.acs.org.

REFERENCES AND NOTES

(1) Burdick, J. A.; Anseth, K. S. *Biomaterials* **2002**, *23*, 4315–4323.
(2) Nguyen, K. T.; West, J. L. *Biomaterials* **2002**, *23*, 4307–4314.
(3) Ishihara, M.; Obara, K.; Ishizuka, T.; Fujita, M.; Sato, M.; Masuoka, K.; Saito, Y.; Yura, H.; Matsui, T.; Hattori, H.; Kikuchi, M.; Kurita, A. *J. Biomed. Mater. Res.* **2003**, *64*, 551–559.
(4) Drury, J. L.; Mooney, D. J. *Biomaterials* **2003**, *24*, 4337–4351.
(5) Hunt, N. C.; Shelton, R. M.; Grover, L. M. *Biomaterials* **2009**, *30*, 6435–6443.
(6) Tan, H. P.; Chu, C. R.; Payne, K. A.; Marra, K. G. *Biomaterials* **2009**, *30*, 2499–2506.
(7) Liu, Y. X.; Chan-Park, M. B. *Biomaterials* **2010**, *31*, 1158–1170.
(8) Liu, Y. X.; Chan-Park, M. B. *Biomaterials* **2009**, *30*, 196–207.
(9) Elisseeff, J.; McIntosh, W.; Anseth, K.; Riley, S.; Ragan, P.; Langer, R. *J. Biomed. Mater. Res.* **2000**, *51*, 164–171.
(10) Nuttelman, C. R.; Tripodi, M. C.; Anseth, K. S. *Matrix Biol.* **2005**, *24*, 208–218.
(11) Shen, J. Y.; Chan-Park, M. B.; He, B.; Zhu, A. P.; Zhu, X.; Beuerman, R. W.; Yang, E. B.; Chen, W.; Chan, V. *Tissue Eng.* **2006**, *12*, 2229–2239.
(12) Mjahed, H.; Porcel, C.; Senger, B.; Chassepot, A.; Netter, P.; Gillet, P.; Decher, G.; Voegel, J.-C.; Schaaf, P.; Benkirane-Jessel, N.; Boulmedais, F. *Soft Matter* **2008**, *4*, 1422–1429.
(13) Grossin, L.; Cortial, D.; Saulnier, B.; Félix, O.; Chasspot, A.; Decher, G.; Netter, P.; Gillet, P.; Mainard, D.; Voegel, J.-C.; Benkirane-Jessel, N. *Adv. Mater.* **2009**, *21*, 650–655.
(14) Tomme, S. R.; Storm, G.; Hennick, W. E. *Int. J. Pharm.* **2008**, *355*, 1–18.
(15) Kopeček, J.; Yang, J. *Polym. Int.* **2007**, *56*, 1078–98.

(16) Recum, H. A.; Kim, S. W.; Kikuchi, A.; Okuhara, M.; Sakurai, Y.; Okano, T. *J. Biomed. Mater. Res.* **1998**, *40*, 631–639.

(17) Liu, R. X.; Fraylich, M.; Saunders, B. R. *Colloid Polym. Sci.* **2009**, *287*, 627–643.

(18) Wanka, G.; Hoffmann, H.; Ulbricht, W. *Colloid Polym. Sci.* **1990**, *268*, 101–117.

(19) Wang, P.; Johnston, T. P. *J. Appl. Polym. Sci.* **1991**, *43*, 283–292.

(20) Zhang, M.; Li, X. H.; Gong, Y. D.; Zhao, N. M.; Zhang, X. F. *Biomaterials* **2002**, *23*, 2641–2648.

(21) VandeVord, P. J.; Matthew, H. W. T.; DeSilva, S. P.; Mayton, L.; Wu, B.; Wooley, P. H. *J. Biomed. Mater. Res.* **2002**, *59*, 585–590.

(22) Varghese, S.; Elisseff, J. H. *Adv. Polym. Sci.* **2006**, *203*, 95–144.

(23) Mu, Q.; Fang, Y. E. *Carbohydr. Polym.* **2008**, *72*, 308–314.

(24) Recillas, M.; Silva, L. L.; Peniche, C.; Goycoolea, F. M.; Renaudo, M.; Argüelles-Monal, W. M. *Biomacromolecules* **2009**, *10*, 1633–1641.

(25) Mao, Z. W.; Ma, L.; Yan, J.; Yan, M.; Gao, C. Y.; Shen, J. C. *Biomaterials* **2007**, *28*, 4488–4500.

(26) Dang, J. M.; Sun, D. N. D.; Shin-Ya, Y.; Sieber, A. N.; Kostuik, J. P.; Leong, K. W. *Biomaterials* **2006**, *27*, 406–418.

(27) Tang, Y. F.; Du, Y. M.; Hu, X. W.; Shi, X. W.; Kennedy, J. F. *Carbohydr. Polym.* **2007**, *67*, 491–499.

(28) Chung, H. J.; Bae, J. W.; Park, H. D.; Lee, J. W.; Park, K. D. *Macromol. Symp.* **2005**, *224*, 275–286.

(29) Chenite, A.; Chaput, C.; Wang, D.; Combes, C.; Buschmann, M. D.; Hoemann, C. D.; Leroux, J. C.; Atkinson, B. L.; Binette, F.; Selmani, A. *Biomaterials* **2000**, *21*, 2155–2161.

(30) Chen, H. Q.; Fan, M. W. *J. Bioactive Compatible Polym.* **2008**, *23*, 38–48.

(31) Bhattarai, N.; Ramay, H. R.; Gunn, J.; Matsen, F. A.; Zhang, M. Q. *J. Controlled Release* **2005**, *103*, 609–624.

(32) Bhattarai, N.; Matsen, F. A.; Zhang, M. Q. *Macromol. Biosci.* **2005**, *5*, 107–111.

(33) Kim, M. S.; Choi, Y. J.; Noh, I.; Tae, G. *J. Biomed. Mater. Res.* **2007**, *83*, 674–682.

(34) Reining, B.; Keul, H.; Hocker, H. *Polymer* **1999**, *40*, 3555–3563.

(35) Zhu, Y. B.; Chan-Park, M. B. *Analy. Biochem.* **2007**, *363*, 119–127.

(36) Leane, M. M.; Nankervis, R. *Int. J. Pharm.* **2004**, *271*, 241–249.

(37) Curotto, E.; Aros, F. *Anal. Biochem.* **1993**, *211*, 240–241.

(38) Yao, Z.; Zhang, C.; Ping, Q.; Yu, L. *Carbohydr. Polym.* **2007**, *68*, 781–792.

(39) Gardner, K. H.; Blackwell, J. *Biopolymers* **1975**, *14*, 1581–1595.

(40) Ragnhild, J. N. H.; Varum, K. M.; Grasdalen, H.; Tokura, S.; Smidsrod, O. *Carbohydr. Polym.* **1997**, *34*, 131.

(41) Makuska, R.; Gorochovceva, N. *Carbohydr. Polym.* **2006**, *64*, 319–327.

(42) Gorochovceva, N.; Makuska, R. *Eur. Polym. J.* **2004**, *40*, 685–691.

(43) Nada, A. M. A.; El-Sakhawy, M.; Kamel, S.; Eid, M. A. M.; Adel, A. M. *Carbohydr. Polym.* **2006**, *63*, 113–121.

(44) Decker, C. *Macromol. Rapid Commun.* **2002**, *23*, 1067–1093.

(45) Discher, D. E.; Janmey, P.; Wang, Y. L. *Science* **2005**, *310*, 1139–1143.

(46) Engler, A. J.; Sen, S.; Sweeney, H. L.; Discher, D. E. *Cell* **2006**, *126*, 677–689.

(47) Kocgozlu, L.; Lavalle, P.; Koenig, G.; Senger, B.; Haikel, Y.; Schaaf, P.; Voegel, J.-C.; Tenenbaum, H.; Vautier, D. *J. Cell Sci.* **2010**, *123*, 29–39.

(48) Desai, N. P.; Hubbell, J. A. *J. Biomed. Mater. Res.* **1991**, *25*, 829–843.

(49) Park, K. D.; Okano, T.; Nojiri, C.; Kim, S. W. *J. Biomed. Mater. Res.* **1988**, *22*, 977–992.

(50) Zhang, M. Q.; Desai, T.; Ferrari, M. *Biomaterials* **1998**, *19*, 953–960.

(51) Boudou, T.; Crouzier, T.; Ren, K.; Blin, G.; Picart, C. *Adv. Mater.* **2010**, *22*, 441–467.

(52) Feng, J.; Chan-Park, M. B.; Shen, J. Y.; Chan, V. *Tissue Eng.* **2007**, *13*, 1003–1011.

AM1002876

ARTICLE